Non-uniform frequency domain for optimal exploitation of non-uniform sampling

Krzysztof Kazimierczuk [a,b], Anna Zawadzka-Kazimierczuk [a], Wiktor Koźmiński [a,*]

[a] *Faculty of Chemistry, University of Warsaw, Pasteura 1, 02-093 Warsaw, Poland*
[b] *Swedish NMR Centre, University of Gothenburg, Box 465, S-405 30 Gothenburg, Sweden*

ARTICLE INFO

ABSTRACT

Random sampling of NMR signal, not limited by Nyquist Theorem, yields up to thousands-fold gain in the experiment time required to obtain desired spectral resolution. Discrete Fourier transform (DFT), that can be used for processing of randomly sampled datasets, provides rarely exploited possibility to introduce irregular frequency domain. Here we demonstrate how this feature opens an avenue to NMR techniques of ultra-high resolution and dimensionality. We present the application of high resolution 5D experiments for protein backbone assignment and measurements of coupling constants from the 4D E.COSY multiplets. Spectral data acquired with the use of proposed techniques allow easy assignment of protein backbone resonances and precise determination of coupling constants.

1. Introduction

NMR is nowadays one of the most efficient spectroscopic techniques, providing a unique insight into the structure and dynamics of biomolecules.

The widely used procedure which enables obtaining spectra of NMR signals is a very efficient algorithm of fast Fourier transform [1] (FFT). First employed for 1D NMR, it has been used later to process signals of higher dimensionalities treated by a sequential transformation, separate for each dimension. In fact, FFT is a highly numerically efficient algorithm for calculating DFT. However, the price for this efficiency is a strict requirement regarding the shape of time domain data, which states that sampling points must be evenly spaced and their number must be an integer power of 2. This requirement implies the need to fulfill the Nyquist Theorem, which stands that sampling frequency is to be twice as high as the highest frequency expected in the signal. The Nyquist Theorem limits implicitly the maximum acquisition time for a given number of time domain points, and consequently limits the precision of frequency determination. This effect, which manifests itself by increased linewidths, goes up with spectral width and number of dimensions, as the latter are sampled and transformed separately. Thus, the advantage of resolving overlapping peaks by the multidimensional analysis is partially lost due to large linewidths. The problem of sampling-limited experiment time becomes relatively severe comparing to sensitivity limitations overcome by employ-ing cooled probes and high magnetic fields. Moreover, high field magnets provide larger spectral widths and thus require higher Nyquist sampling rates.

Methods that have been developed up to the date to deal with the problem were usually aimed at reducing the measurement time without loss of spectral resolution, whereas those aimed at improving resolution without increasing experiment duration were given much less attention. However, improved resolution is definitely more interesting from a scientific point of view as it may reveal effects that remain hidden when spectral lines are broad [2,3]. Some of the methods proposed in the past are: back-projection reconstruction [4] and multiway decomposition [5] applied for radial sampling, maximum entropy methods [6] and multidimensional decomposition [7] for random sampling, and covariance spectroscopy [8] where extraordinary resolution can be obtained even from truncated conventionally sampled signal. An approach to perform multidimensional experiment in a single scan with spatial encoding was also presented [9].

Although above sophisticated methods of signal processing may improve spectral analysis in several ways, there is no general need to use them in order to obtain spectrum of non-conventionally (radially, randomly, etc.) sampled signal. As we showed before [10] replacing standard multidimensional FFT approach by multidimensional one-step DFT (referred to as multidimensional Fourier transform (MFT)) allows one to estimate [11] the spectrum from such dataset. The estimation error takes form of spectral artifacts, that appear as a consequence of non-orthogonality of Fourier transform (FT) base functions for irregularly sampled signals [12]. The artifacts are inherently associated with the peaks, i.e. they

* Corresponding author. Fax: +48 22 822 5996.
E-mail address: kozmin@chem.uw.edu.pl (W. Koźmiński).
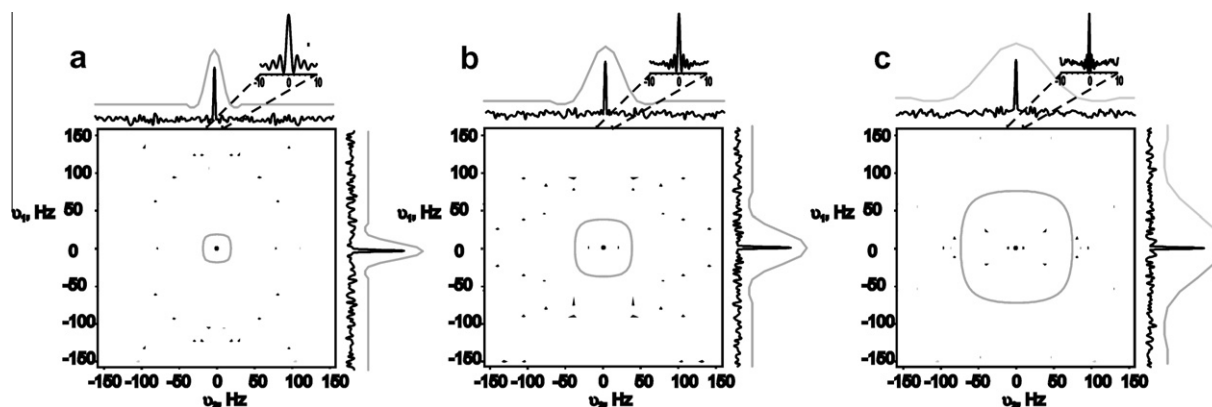
Fig. 1. 2D cross-sections from simulated: (a) 3D, (b) 4D, (c) 5D spectra. The threshold was set at 10% of peak intensity; 256 time points were generated randomly with uniform distribution and maximum evolution time of 0.4 s (panel a), 0.8 s (panel b) and 1.6 s (panel c), in all dimensions. The distance between spectral points was set at 1/maximum evolution time to hide the effect of signal truncation. The inserts showing a spectral line narrowing obtained by MFT using higher digital resolution. Simulation was repeated for the conventional set of 256 points, with the Nyquist rate of 16×16 (panel a), $8 \times 8 \times 4$ (panel b), and $4 \times 4 \times 4 \times 4$ (panel c). Peaks obtained in such way are shown with grey line.

are part of point spread function (PSF) of the sampling schedule. Convolution of the PSF with the FT of a perfect, continuous signal gives the actually observed spectrum of randomly sampled signal. The presence of the artifacts is thus the price to pay for narrowed peak widths or increased dimensionality obtainable by the random sampling. Whereas the MFT can be performed using any set of samples, the best way is to sample the time domain randomly [13]. In such case the artifacts reveal similar properties as thermal noise [14], i.e. they are spread evenly in the frequency domain and the relative signal-to-artifact ratio depends only on the square root of number of samples, but not on the dimensionality nor maximum evolution time. This suggests that the proposed method should be used for designing novel experiments with large (in terms of both: maximum time and dimensionality) evolution time domain, rather than to shorten the duration of standard experiments (Fig. 1).

2. Methods

Besides the ability to process a non-uniformly sampled time domain dataset, MFT allows similar non-uniformity in the frequency domain i.e. Fourier integral can be calculated for arbitrary chosen frequency coordinates. This feature opens way to better exploitation of NMR experiments providing spectra of high dimensionality or ultra-narrow peaks that would require hundreds of gigabytes of disk space, if transformed to the regular frequency domain spectral matrix (not to mention the numerical cost of such operation). Because peaks in NMR spectra are relatively rare, it is possible to limit calculations to reasonably small regions of interest. Such regions of spectrum, that one wants to visualize can be chosen basing on

some a priori knowledge and obtained using a variant of MFT referred to as sparse MFT (SMFT). Idea of the sparse MFT can be exploited in various ways – two of them are presented below.

Firstly, one can exploit the idea that is the essence of common approach to analysis of multidimensional NMR data i.e. consecutive examination of various spectra. Peak locations in some of spectral dimensions of 4D or 5D spectra are usually known from spectra of lower dimensionality (2D, 3D) acquired at early stages of NMR analysis. Thus, frequency coordinates in these dimensions can be set to the exact peak frequencies during transformation (see example 1) and only low-dimensional cross-sections of full 4D or 5D spectrum are to be calculated [15]. Such cross-sections (see Fig. 2) facilitate the assignment of spectral peaks to the particular nuclei in the protein backbone.

Some NMR techniques allow one to observe even minor internuclear couplings visible as subtle splittings of the respective spectral lines [2,3]; these couplings can be precisely measured only for peaks of width that is practically unattainable using the conventional sampling (in NMR spectra of high dimensionality). Again, the possibility of introducing irregularity in frequency domain allows ultra-high numerical resolution even in such spectra of high dimensionality. A priori knowledge of all frequency coordinates for each peak allows one to calculate only these spectral regions, that contain peaks (see example 2). In this case the peak coordinates do not need to be accurate. Because the transformed regions can be very narrow (tens of Hz), ultra-high numerical resolution (few Hz per spectral point) can be easily achieved. The benefit of reaching natural, relaxation-limited linewidths, that is enabled by the random sampling, can be fully exploited with this method, as
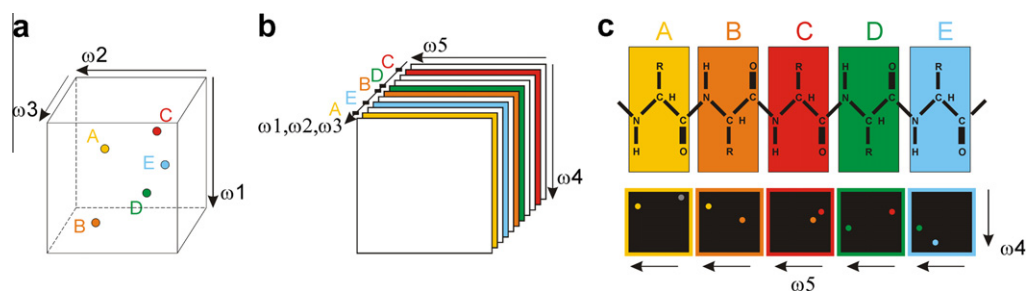
Fig. 2. Calculation of a set of 2D cross-sections of 5D spectrum – example of SMFT application. (a) Scheme of 3D spectrum with a few peaks; (b) scheme of 5D spectrum; three dimensions ω_1, ω_2 and ω_3, which correspond to nuclei observed in 3D spectrum are symbolized by one axis, two other dimensions (ω_4 and ω_5) are shown on separate axes. Only 2D (ω_4–ω_5) cross-sections that contain peaks are calculated in SMFT (marked with colors), basing on ω_1, ω_2 and ω_3 frequency coordinates of peaks from 3D spectrum. (c) Scheme of 2D cross-sections of 5D spectrum, calculated for ω_1, ω_2 and ω_3 coordinates equal to positions of peaks in 3D spectrum. Shown cross-sections correspond to consecutive amino acids in protein chain.
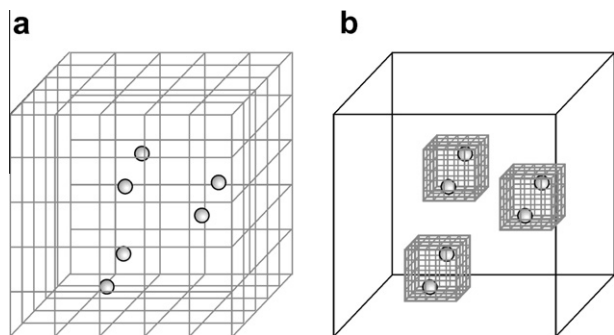
Fig. 3. Three-dimensional scheme showing the gain on digital resolution with the use of "cube" S-MFT: (a) full "spectrum" with ultra-narrow peaks spitted into E.COSY multiplets. The digital resolution of discrete frequency space (grey lines) is too small to properly approximate so narrow peaks and (b) spectral "cubes" obtained by SMFT feature much better digital resolution than full spectrum and allow proper visualization of spectral multiplets. It should be emphasized, that the "cube" SMFT is used in the four-dimensional version in this work.

shown in Fig. 3. Thus, an information on additional spectral parameters dependent on molecular structure can be obtained.

### 2.1. The sparse MFT procedure

The extremely narrow, high-dimensional spectral peaks need increased digital resolution (or lower number of Hz per spectral point) to be properly visualized. Even with the minimal number of three points per peak in each spectral dimension, the resulting amount of spectral data would be in the most cases at least tens of GB large, which is so far impractical. Thus, to effectively exploit the advantages of large evolution time domain, the irregularity of frequency domain should be introduced. There are many practically possible schemes for such procedure, two of them are used to obtain spectra presented in this work and discussed in details below. Both require a priori knowledge of peak coordinates in some (example 1) or all (example 2) of spectral dimensions. This information can be acquired using spectra of lower dimensionality, typically 2D ^{15}N-HSQC, 3D HNCO, 3D HNCA or their combinations. Especially useful is HNCO experiment due to excellent peak dispersion, lack of significant homonuclear couplings, and good relaxation properties even for large proteins [16].

3. Experiments and results

3.1. "Slice" SMFT

Usually, the spectra used for the backbone assignment are analyzed after an initial peak-picking of 2D ^{15}N-HSQC or 3D HNCO. Initial information about chemical shifts of amide ^{1}H and ^{15}N nuclei (optionally also carbonyl ^{13}C nuclei) allows consequently more optimal exploration of high-dimensional spectral space in order to localize peaks and determine chemical shifts of other nuclei involved in coherence transfer. This idea can be exploited not only during spectral analysis, but also one-step earlier i.e. during FT. "Slow" DFT (not employing Cooley-Tukey FFT algorithm) allows arbitrary setting of some frequency coordinates during the transformation of multidimensional signal. They can be out of a conventional regular frequency grid e.g. equal to resonance frequencies of peaks from a spectrum of lower dimensionality. Instead of a fully dimensional spectrum one obtains lower-dimensional cross-sections, that are much more convenient to be handled, due to much smaller computational and disk space requirements. As we presented before [15], such set of spectral cross-sections opens new possibilities for efficient backbone assignment algorithms. The whole transformation and assignment procedure is described below, using example of 5D HN(CA)CONH experiment.

1. Perform 3D HNCO experiment, preferably employing random sampling to obtain spectrum of high resolution in reasonable time.
2. Prepare list of HNCO peaks (not assigned).
3. Perform 5D HN(CA)CONH experiment using random sampling, set the maximum evolution times high enough to obtain satisfactory linewidths, regarding transverse relaxation rates.
4. Calculate a set of 2D cross-sections ($H'_N - N'_H$) of 5D spectrum, for H_N, N_H and CO coordinates known from HNCO peak list. Number of cross-sections is equal to number of peaks in the HNCO peak list (ca. number of amino acids in protein, excluding prolines).
5. Find sequential connections: On each cross-section two cross-peaks of an opposite sign, originating from amide groups of adjoining amino acids, are expected. Thus, for spectral cross-sections corresponding to two adjoining residues, one peak is common and therefore sequential connections can be
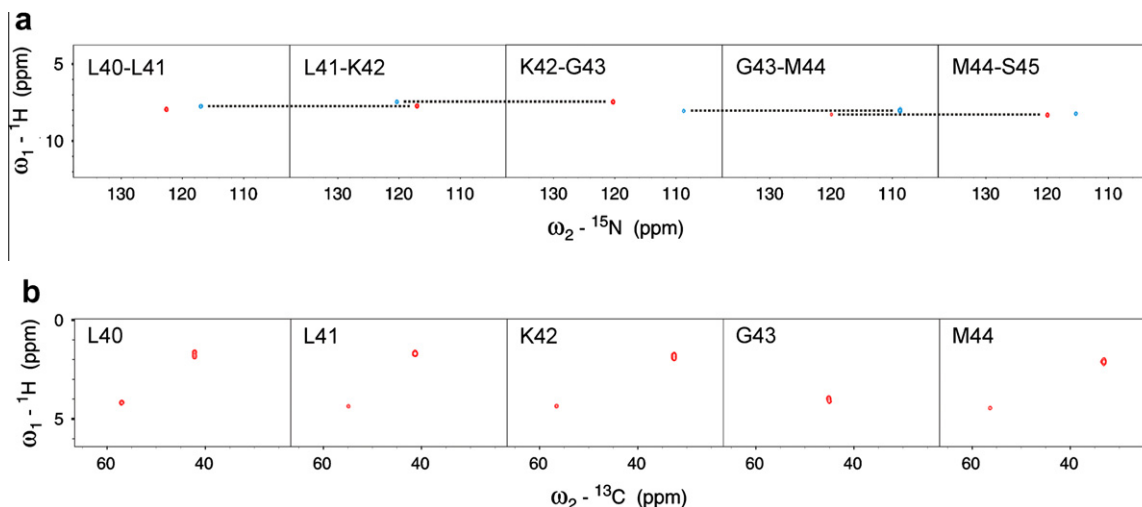
Fig. 4. The experimental example of ultra-high resolution multidimensional NMR spectra acquired for 5–79 fragment of bovine Ca^{2+}-loaded Calbindin protein. Cross-sections for consecutive amino acids obtained by the SMFT are presented (fragment L40 – S45). Each experiment lasted for 17 h. For experimental parameters, complete set of 2D cross-sections and pulse sequences details see Supplementary Material. (a) 2D HN–NH cross-sections of 5D HN(CA)CONH experiment. Inter-residual links facilitating signal assignment are marked with dotted lines. For glycine residues the sign of cross-peaks is reversed. (b) 2D H$_{\alpha\beta}$–C$_{\alpha\beta}$ cross-sections of 5D HabCabCONH experiment.
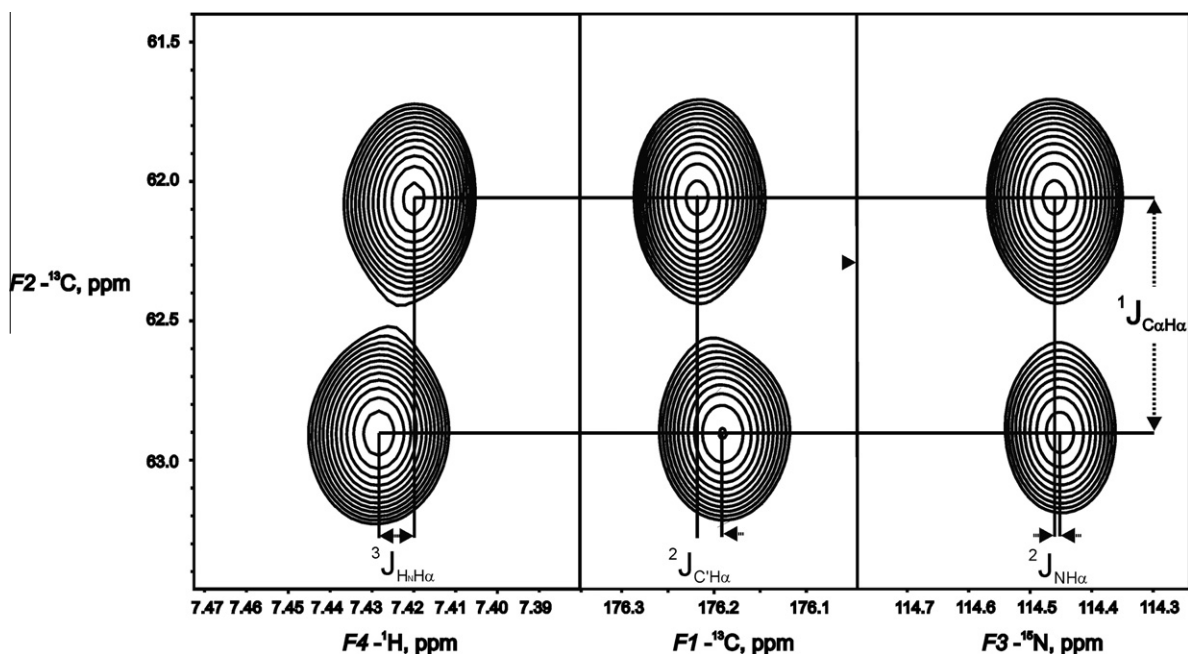
Fig. 5. The experimental example of ultra-high resolution multidimensional NMR spectra obtained by the proposed technique: I74 intra-residual resonance from 89-h 4D HNCACO-{H$_\alpha$}-coupled experiment acquired for 5–79 fragment of bovine Ca^{2+}-loaded Calbindin protein. Depicted cross-sections of 4D "cube" $50 \times 450 \times 40 \times 100$ Hz surrounding the peak allow determination of coupling constants from resolved 4D E.COSY pattern. $^1J_{C\alpha H\alpha}$ = 135.9 Hz, $^3J_{HNH\alpha}$ = 5.8 Hz, $^2J_{C'H\alpha}$ = −5.0 Hz, $^2J_{NHH\alpha}$ = −1.0 Hz with numerical resolution of 0.4 Hz/point, 1.7 Hz/point, 0.2 Hz/point and 0.7 Hz/point in dimensions F$_1$, F$_2$, F$_3$ and F$_4$, respectively. For full set of spectral "cubes" from 4D HNCACO-{H$_\alpha$}-coupled and 4D HNCOCA see Supplementary Material.

Table 1
Experimental parameters – experiments for assignment of protein backbone.

Experiment	5D HN(CA)CONH					5D HabCabCONH				
Number of sampling points	675					725				
Number of transients	4					4				
Experiment time	17 h					18 h				
Corresponding conv. exp. time	ca. 11 years					ca. 54 years				
Number of calculated cross-sections (peaks)	71					71				
Computing time	1.5 min[a]/2.5 h[b]					1.9 min[a]/3 h[b]				
Spectral parameters for SMFT	H'_N	N'_H	CO	N$_H$	H$_N$	H$_{\alpha\beta}$	C$_{\alpha\beta}$	CO	N$_H$	H$_N$
Number of real spectral points	112	224	nop	nop	nop	96	320	nop	nop	nop
Spectral width, kHz	6	2.5	set	set	set	4	14	set	set	set
Maximum evolution time, ms	5.5	27.5	8.9	27.5	85	6.5	7.1	28	28	85

nop – equal to number of peaks.
set – frequency coordinate set to peak resonance frequency.
Peak coordinates were determined on the basis of 3D HNCO experiment.
Computing time – time of calculations on single CPU, 1.6 GHz, 8 GB RAM:
  [a] Calculation time of SMFT.
  [b] Calculation time of algorithm of random sampling artifacts suppression [24], for example of cleaning procedure see Supplementary material Fig. S6.

established (see Fig. 4, full set of cross-sections is given in Supplementary Material). Such procedure allows to link big fragments of a protein backbone (between proline residues).

6. Assign peaks to appropriate spin system in polypeptide chain: Length of the linked fragments usually indicates the position in protein chain where the fragment fits. Additionally, in the case of HN(CA)CONH experiment cross-peaks signs can be used to verify assignment. When coherence is transferred via C$_\alpha$ of glycine residue, the signs are reversed.

3.2. "Cube" SMFT

As mentioned before, maximum evolution times in NMR experiment employing random sampling may be extended without increasing artifact level in spectra obtained by MFT. This allows novel experiments resulting in spectra featuring ultra-narrow peaks and revealing effects of subtle physical interactions, e.g. small scalar couplings. Recently, we have described the 3D HNCO-{C$_\alpha$}-coupled experiment, where three-dimensional E.COSY [17] multiplet structure of spectral peaks was observed [3]. In this work we present experiments that allow observation of four-dimensional E.COSY pattern. However, obtaining full spectrum featuring such a high dimensionality and such narrow peaks is practically impossible using standard sequential FFT approach, due to requirement of high digital resolution. Again, the irregularity of frequency domain needs to be introduced – only some (but fully-dimensional) regions ("cubes", see Fig. 3) of the spectrum are calculated basing on a priori knowledge of approximate peak positions in all dimensions. For example, the "cube" version of SMFT may be introduced for the analysis of 4D HNCACO-{H$_\alpha$}-coupled signal in the following way:

Table 2
Experimental parameters – experiments for J-coupling measurements.

| Experiment	4D HNCACO-{H$_\alpha$}-coupled				4D HNCOCA-{C$_\beta$}-coupled			
Number of sampling points	7000				1300			
Number of transients	4				4			
Experiment time	89 h				17 h			
Corresponding conv. exp. time	ca. 2.5 years				ca. 39 years			
Number of "cubes" (peaks)	138				71			
Computing time	169 h				5.5 h			
Spectral parameters of the "cube" for SMFT on all peaks	H$_N$	N$_H$	CO	C$_\alpha$	H$_N$	N$_H$	CO	C$_\alpha$
M_{loc}	32	32	32	64	16	128	32	32
sw$_{loc}$, Hz	60	40	50	450	100	80	100	200
Digital res., Hz/pts	1.88	1.25	1.56	7.03	6.25	0.63	3.13	6.25
Linewidth, Hz	24	12.5	20	100	22	7.8	10.2	26.5

M_{loc} – number of real spectral points.
sw$_{loc}$ – size of cube ("local" spectral width).
Line width is average half-width of the peak, predicted basing on maximum evolution time and average relaxation rate.
Peak coordinates were determined on the basis of HNCA and HNCO experiments.
Computing time – time of calculations on single CPU, 1.6 GHz, 8 GB RAM. Contrary to other MFT packages, "cube" computations are not well optimized yet.
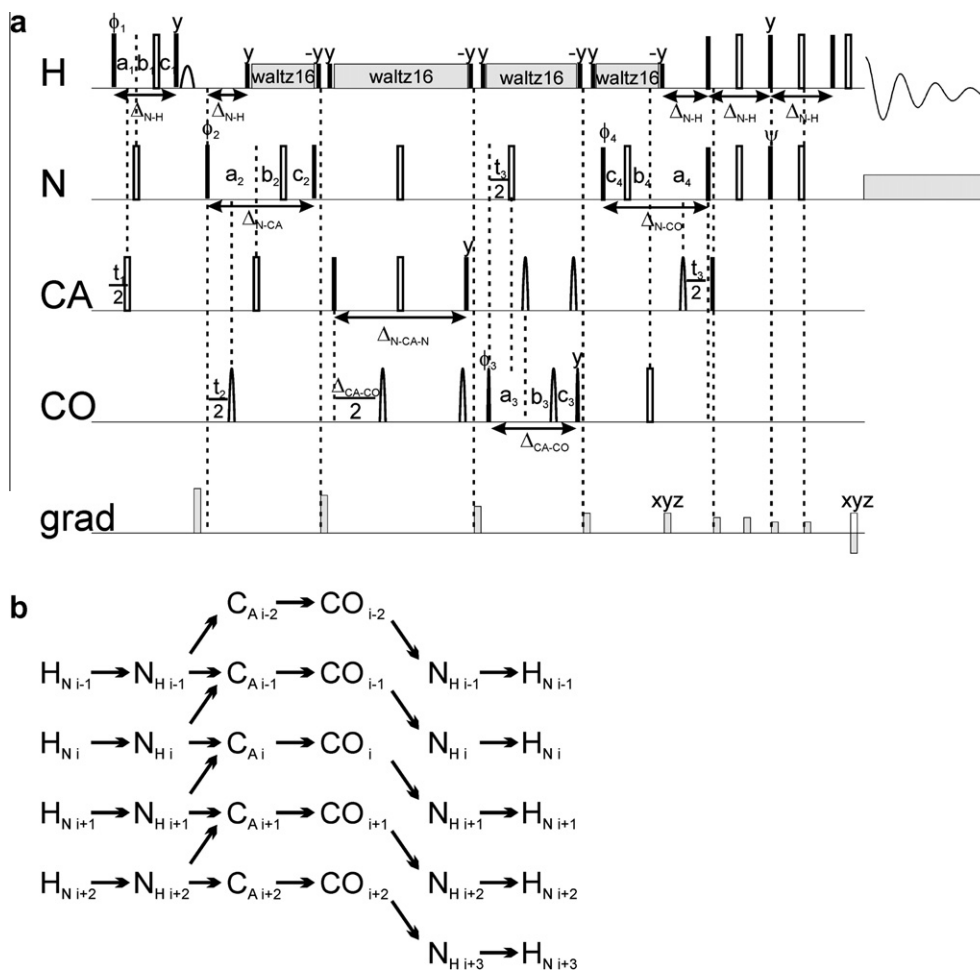
Fig. 6. Pulse sequence of the 5D HN(CA)CONH technique: (a) pulse sequence diagram and (b) scheme of coherence transfer pathway. Amide proton, carbon CO and both amide nitrogen evolution delays are in semi-constant-time mode ($a_i = (t_i + \Delta)/2$, $b_i = t_i(1 - \Delta/t_i^{max})/2$, $c_i = \Delta(1 - t_i/t_i^{max})/2$) or in constant-time mode ($a_i = (\Delta + t_i)/2$, $b_i = 0$, $c_i = (\Delta - t_i)/2$), where Δ stands for Δ_{N-H}, Δ_{CA-CO} and Δ_{N-CA}, respectively, t_i is the ith point from random sampling schedule and t_i^{max} is maximal length of the delay. Delays were set as follows: Δ_{N-H} = 5.4 ms, Δ_{N-CA} = 28 ms, Δ_{N-CA-N} = 28.6 ms, Δ_{CA-CO} = 9.1 ms and Δ_{N-CO} = 28 ms. Coherence selection gradients (marked by xyz) were applied at magic angle. This pulse sequence is analog of the 6D APSY HNCOCANH experiment [22], however the CA and CO evolutions periods are swapped in order to enable calculation of $\omega_1 - \omega_2$ cross-sections with to signals per each H,N, CO set of coordinates from the HNCO spectrum.

1. 4D list of predicted spectral peak coordinates is prepared basing on 3D HNCO and 3D HNCA experiments (the list containing CO^i, C$_\alpha^i$, N$_H^i$, H$_N^i$ and CO^{i-1}, C$_\alpha^{i-1}$, N$_H^i$, H$_N^i$ chemical shifts should be con-structed). Peak positions do not have to be exact; in practice they may vary up to tens of Hz, depending on the "local" spectral width set (see point 2).

2. "Local" spectral widths and numbers of spectral points for each dimension of the "cube" are chosen. The number of "cubes" will be equal to the number of peaks in the 4D list prepared before. Center of each "cube" is defined by peak coordinates from the list. The "local" spectral widths and the number of spectral points are the same for each "cube" and define the spectral space in the same (regular, on-grid) way as for full conventional spectrum. Typical values of "local" spectral widths and numbers of spectral points are presented in Table 2.

3. Spectral "cubes" are obtained by SMFT of the 4D HNCACO-$\{H_\alpha\}$-coupled signal sampled randomly. Multidimensional Fourier transform is performed in a standard way, the only exception is the shape of frequency space which is limited to relatively small cubes featuring high digital resolution. This does not affect the algorithm of transformation, as it allows irregularity of both: frequency and time space by definition. The example of 4D E.COSY pattern obtained in HNCACO-$\{H_\alpha\}$ experiment is given in Fig. 5. For full set of spectral "cubes" – see Supplementary Material (because of visualization limitations, only 2D cross-sections of cube are presented).

4. Discussion

The recently introduced [15] approach to non-uniform frequency space (i.e. SMFT), based on Fourier transform, was generalized and combined with three novel NMR techniques dedicated for use with SMFT. The application of random sampling in 5D HN(CA)CONH, 5D HabCabCONH and 4D HNCACO-$\{H_\alpha\}$ experiments allowed to reach extraordinary peak dispersion, which can be fully exploited only if appropriate digital resolution can be used during processing. Use of non-uniform frequency domain is essential here, as it reduces the amount of spectral data and the computational time even millions of times comparing to full spectrum of the same digital resolution.

5. Experimental

All spectra were acquired for 1.0 mM sample of $^{13}C,^{15}N$-labelled 5–79 fragment of bovine Ca^{2+}-loaded Calbindin d9 k P47 M mutant at 250 C with pH = 6.0 in 9:1 H_2O/D_2O obtained from Protera (www.protera.it) on a Varian NMR System 700 spectrometer equipped with a Performa XYZ PFG unit, using the standard 5 mm ^1H, ^{13}C, ^{15}N – triple resonance probehead. High power ^1H, ^{13}C, and ^{15}N $\pi/2$ pulses of 5.4, 13.5, and 31.0 μs, respectively, were used. Selective CA and CO pulses were realized as phase modulated (for off-resonance excitation or inversion) *sinc* shapes, with B_1 field strength adjusted to have a minimal effect on CO and CA, respectively. The selective H_N pulses in HNCACO-$\{H_\alpha\}$-coupled sequence were realized using ReBURP shapes [18]. In all cases, four scans per each data set with the acquisition time of 85 ms and relaxation delay of 1.2 s were set. For processing of a directly detected dimension cosine square weighting function was applied prior to Fourier transformation with zero-filling to 1024 complex points. For other experimental parameters see Tables 1 and 2. The pulse sequences were developed using own-developed programming library. HNCACO-$\{H_\alpha\}$-coupled pulse sequence was derived from HN(CA)CO [19], by using selective refocusing of amide protons instead of broad-band ^1H decoupling and extended to 4D. The 4D HNCOCA pulse sequence, with HSQC-type CO–CA coherence transfer, was obtained by extension of standard 3D HN(CO)CA [20], and
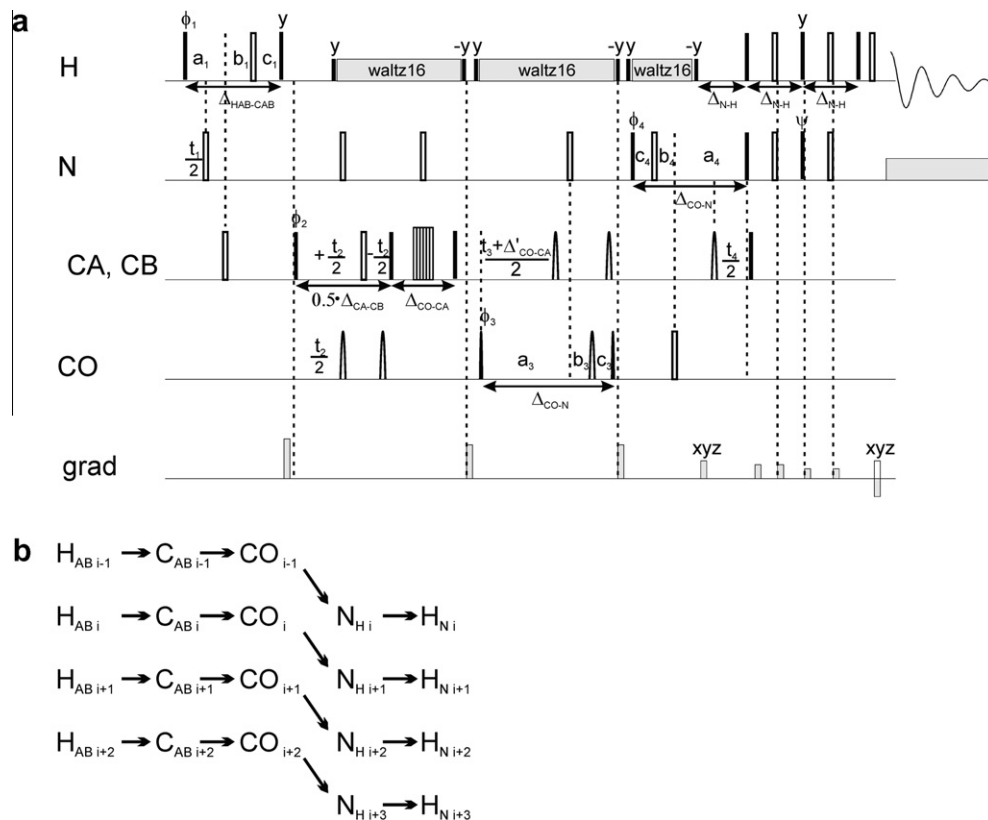
Fig. 7. Pulse sequence of 5D HabCabCONH technique: (a) pulse sequence diagram and (b) scheme of coherence transfer pathway. Proton $H_{\alpha\beta}$, carbon CO and amide nitrogen evolution delays are in semi-constant-time mode: $a_i = (t_i + \Delta)/2$, $b_i = t_i(1 - \Delta/t_i^{max})/2$, $c_i = \Delta(1 - t_i/t_i^{max})/2$ (where Δ stands for $\Delta_{HAB-CAB}$, Δ_{CO-N} and Δ_{CO-N}, respectively, t_i is the ith point from a random sampling schedule and t_i^{max} is maximal length of the delay), carbon $C_{\alpha\beta}$ evolution delays are in the constant-time mode ($\pm \frac{t_2}{2}$ means $\frac{0.5 \cdot \Delta_{CA-CB} \pm t_2}{2}$). Delays were set as follows: $\Delta_{HAB-CAB} = 3.6$ ms, $\Delta_{CA-CB} = 14.3$ ms, $\Delta_{CO-CA} = 6.8$ ms, $\Delta'_{CO-CA} = 9.1$ ms, $\Delta_{CO-N} = 28$ ms, $\Delta_{N-H} = 5.4$ ms. Refocusing of C_α and inversion of CO spins was achieved using 6-element composite pulse [23]. The coherence selection gradients (marked by xyz) were applied at the magic angle.

adapted to random sampling. Diagrams of 5D HN(CA)CONH and 5D HabCabCONH pulse sequences and corresponding coherence transfer pathways are given in Figs. 6 and 7.

The data was processed using the SMFT software available from the authors. The resulting spectra were displayed and analyzed using SPARKY software [21].

6. Conclusions

All said, we believe that the irregular (or sparse) MFT offers a convenient and highly useful approach for processing the randomly sampled NMR signals of high dimensionality, yielding spectra of unsurpassed resolution. Random sampling can be easily implemented on any spectrometer. MFT does not require more user-defined parameters than conventional FT, and can be performed on a single standard PC computer; the MFT software needed is available on request from the authors.

Acknowledgments

Appendix A. Supplementary data

Supplementary data associated with this article can be found in the online version, at doi:10.1016/j.jmr.2010.05.012.

References

[1] J.W. Cooley, J.W. Tukey, An algorithm for machine calculation of complex Fourier series, Math. Comput. 19 (1965) 297–301.
[2] D.A. Snyder, Y. Xu, D. Yang, R. Bruschweiler, Resolution-enhanced 4D 15N/13C NOESY protein NMR spectroscopy by application of the covariance transform, J. Am. Chem. Soc. 129 (2007) 14126–14127.
[3] K. Kazimierczuk, A. Zawadzka, W. Kozminski, I. Zhukov, Determination of spin−spin couplings from ultrahigh resolution 3D NMR spectra obtained by optimized random sampling and multidimensional Fourier transformation, J. Am. Chem. Soc. 130 (2008) 5404–5405.
[4] Ē. Kupče, R. Freeman, Projection–reconstruction of three-dimensional NMR spectra, J. Am. Chem. Soc. 125 (2003) 13958–13959.
[5] D. Malmodin, M. Billeter, Multiway decomposition of NMR spectra with coupled evolution periods, J. Am. Chem. Soc. 127 (2005) 13486–13487.
[6] A.S. Stern, J.C. Hoch, Maximum entropy reconstruction in NMR. In: D.M. Grant, R. Harris (Eds.), In: Encyclopedia of Nuclear Magnetic Resonance, Vol. 8, John Wiley & Sons, Chichester, UK, 1996.
[7] V.Y. Orekhov, I. Ibraghimov, M. Billeter, Optimizing resolution in multidimensional NMR by three-way decomposition, J. Biomol. NMR 27 (2003) 165–173.
[8] F.L. Zhang, R. Bruschweiler, Indirect covariance NMR spectroscopy, J. Am. Chem. Soc. 126 (2004) 13180–13181.
[9] L. Frydman, T. Scherf, A. Lupulescu, The acquisition of multidimensional NMR spectra within a single scan, Proc. Natl. Acad. Sci. USA. 99 (2002) 15858–15862.
[10] K. Kazimierczuk, W. Koźmiński, I. Zhukov, Two-dimensional Fourier transform of arbitrarily sampled NMR data sets, J. Magn. Reson. 179 (2006) 323–328.
[11] A. Tarczyński, N. Allay, Spectral analysis of randomly sampled signals: suppression of aliasing and sampler jitter, IEEE Trans. Signal Process. 52 (2004) 3324–3334.
[12] I. Bilinskis, Digital Alias-free Signal Processing, Wiley, 2007.
[13] K. Kazimierczuk, A. Zawadzka, W. Koźmiński, I. Zhukov, Random sampling of evolution time space and Fourier transform processing, J. Biomol. NMR 36 (2006) 157–168.
[14] K. Kazimierczuk, A. Zawadzka, W. Koźmiński, Narrow peaks and high dimensionalities: exploiting the advantages of random sampling, J. Magn. Reson. 197 (2009) 219–228.
[15] A. Zawadzka-Kazimierczuk, K. Kazimierczuk, W. Koźmiński, A set of 4D NMR experiments of enhanced resolution for easy resonance assignment in proteins, J. Magn. Reson. 202 (2010) 109–116.
[16] M. Sattler, J. Schleucher, C. Griesinger, Heteronuclear multidimensional NMR experiments for the structure determination of proteins in solution employing pulsed field gradients, Prog. NMR Spectrosc. 34 (1999) 93–158.
[17] C. Griesinger, O.W. Sorensen, R.R. Ernst, Two-dimensional correlation of connected NMR transitions, J. Am. Chem. Soc. 107 (1985) 6394–6396.
[18] H. Geen, R. Freeman, Band-selective radiofrequency pulses, J. Magn. Reson. 93 (1991) 93–141.
[19] R.T. Clubb, V. Thanabal, G. Wagner, A Constant time three-dimensional triple resonance pulse scheme to correlate intraresidue HN, 15N and 13C′ chemical shifts in 15N–13C labeled proteins, J Magn. Reson. 97 (1992) 213–217.
[20] A. Bax, M. Ikura, An efficient three-dimensional NMR technique for correlating the proton and nitrogen backbone amide resonances with the alpha carbon of the preceding residue in uniformly 13C/15N enriched proteins, J. Biomol. NMR 1 (1991) 99–104.
[21] T.D. Goddard, D.G. Kneller, SPARKY 3, University of California, San Francisco.
[22] F. Fiorito, S. Hiller, G. Wider, K. Wüthrich, Automated resonance assignment of proteins: 6D APSY-NMR, J. Biomol. NMR 35 (2006) 27–37.
[23] A.J. Shaka, Composite pulses for ultra-broadband spin inversion, Chem. Phys. Lett. 120 (1985) 201–205.
[24] K. Kazimierczuk, A. Zawadzka, W. Koźmiński, I. Zhukov, Lineshapes and artifacts in Multidimensional Fourier Transform of arbitrary sampled NMR data sets, J. Magn. Reson. 188 (2007) 344–356.